https://doi.org/10.5194/egusphere-2023-2259
Preprint. Discussion started: 8 November 2023

The calcitic test growth rate of Spirillina vivipara (Foraminifera)

Yukiko Nagai[1,2], Katsuyuki Uematsu[3], Briony Mamo[4], Takashi Toyofuku[1,5]

[1]Institute for Extra-cutting-edge Science and Technology Avant-garde Research (X-star), Japan Agency for Marine-Earth Science and Technology (JAMSTEC), Natsushima-cho 2-15, Yokosuka 237-0061, Japan.
[2]National Museum of Nature and Science, 4-1-1 Amakubo, Tsukuba-shi, Ibaraki 305-0005, Japan
[3]Marine Works Japan Ltd., 3-54-1 Oppama-higashi, Yokosuka 237-0063, Japan
[4]School of Natural Sciences, Faculty of Science and Engineering, Macquarie University, NSW, 2109, Australia
[5]Tokyo University of Marine Science and Technology (TUMSAT), 4-5-7, Konan Minato-ku, Tokyo 108-8477, Japany

Correspondence to: Yukiko Nagai (nagai.y@jamstec.go.jp)

Abstract. Foraminiferal~~ groups~~ encompass vastly differing morphologies, ecological preferences and elemental/ isotopic test compositions. ~~For some of these groups,~~ the calcification mechanism is completely unknown, ~~but is likely differing~~ from that of well-studied groups. This study aim~~ed~~ to understand the test growth and calcification rate of *Spirillina vivipara* Ehrenberg, 1843 (Order Spirillinida), and to compare them to other foraminifera species. Spirillinids have a closely coiled spiral chamber like a tube, yet their calcitic microstructure is unique amongst foraminifera. Calcification observations in *S. vivipara* facilitate the estimation of carbonate precipitation rates during active test ~~elongation~~, which are revealed to be independent of the individual's size. ~~We found that S.~~ *vivipara* grows its test in response to food availability, suggesting that calcification directly corresponds to cell growth. Timelapse observations of *S. vivipara* indicate continuous growth, suggesting active growth phases and interspersed rest periods, hinting at potential biological rhythms in the growth and calcification process. We also implemented a 24-hour observation period using Calcein staining, showing calcite precipitation rates of 8.08 μm/hour ~~in *S. vivipara*~~, which correspond to approximately 364 nmol/cm^2/min i.e. 36.4mg/cm^2/min. These rates are higher than those ~~published for~~ other foraminifera and those in most inorganic precipitation experiments. Such high rates in spirillinid foraminifera may explain their distinctive morphology, elemental composition, unusual reproduction and ecological distribution.

1 Introduction

Foraminifera are one of the major carbonate producers in the ocean, and the impact of climate change on their ~~total~~ test production may have important consequences for marine carbon cycling and thereby, atmospheric CO_2 levels (Langer et al., 1997; Langer, 2008; Narayan et al., 2021). In estimating the fluxes of carbon and calcium, and comparing carbonate synthesis capabilities with other organisms, the growth rate of foraminiferal tests is indispensable. Despite this, research focusing on the measurement of test growth rates are still limited.

In previous studies, attempts have been made to estimate the rate of calcium carbonate production per unit of time in foraminiferal species such as *Archaias angulatus* (Fichtel and Moll, 1798) (Duguay and Taylor, 1978) *Trilobatus sacculifer*

https://doi.org/10.5194/egusphere-2023-2259
Preprint. Discussion started: 8 November 2023

(Brady, 1877) (Erez and Luz, 1982; Anderson and Faber, 1984), *Amphistegina lobifera* Larsen 1976 (Ter Kuile and Erez, 1984), and *Ammonia tepida* (Cushman, 1926) (Glas et al., 2012; Geerken et al., 2022). However, the sporadic and intermittent nature of test growth, coupled with the difficulties in observing test formation, has resulted in a fragmented picture of calcification rates. Moreover, studies that analyse precipitation rate as a function of environmental parameters (e.g. temperature or pH) are lacking.

Spirillinid ~~foraminifera is~~ characterized by a unique mode of test growth, wherein instead of a spiraling chambered whorl form found in Rotaliid foraminifera, these foraminifera consist of a singular, continuous, enrolled, elongate tube (Loeblich and Tappan, 1987). If nutritional conditions are favorable, spirillinids can ~~transition to their next generation~~ in just 7–10 days (Myers, 1936) continuous enrolled tubular morphology, ~~*S.*~~ *vivipara* is classified under Tubothalamea, Spirillinida (Hayward, 2023). Compared to many other benthic foraminifera whose life cycles typically range from two months to several years (Lee and Anderson, 1991; Goldstein, 2003), the life cycle of *Spirillina* is notably short. While many foraminifera release gametes during sexual reproduction, ~~this species~~ forms a zygote through the fusion of two or three ~~gamonts, wherein sexual reproduction occurs~~. Consequently, the geographical dispersion of this species is anticipated to occur not through the gametes radiation but rather in an already juvenile state. This suggests that the species primarily disperses through propagules (Alve and Goldstein, 2010; Murray, 2013). In this study, we used *S. vivipara* to observe test growth and measure test extension rate through laboratory cultivation experiments. Based on these results, we have been able to estimate the calcitic precipitation rates of the species. Furthermore, to understand the degree by which the presence or absence of food impacts test growth, we also ran ~~the~~ experiment under a 72-hour fasting scenario.

2 Materials and Methods

2.1 Sample Collection and Lab Culture

Samples of living *S. vivipara* specimens were collected amongst flourishing algae from the eelgrass tank of the New Enoshima Aquarium in July 2017 and December 2018 for culture experiments. The algae were brought to JAMSTEC headquarters in Yokosuka, where specimens of *S. vivipara* were handpicked using an eyelash and cultured in Petri dishes. Living specimens were identified by the circulation of cytoplasm and the presence of pseudopodia. Any extraneous sediment or debris was removed under a stereoscopic microscope (SteREO Discovery.V12, Zeiss Co. Ltd.) and transferred into filtered natural seawater with a salinity of 35±0.1. Specimens were cultured in glass Petri dishes of 45 mm-diameter, maintained at 23±0.5°C, and small amounts of live microalgae (*Dunaliella tertiolecta*, NIES-2258) were added twice a week.

2.2 Test Formation Observation

Two measurement methodologies were applied in this study. One involved capturing continuous time-lapse images to measure the test extension per unit of time. The other involved introducing the fluorescent reagent Calcein at the start of the experiment to mark the test, and then measured the length of the test after a prescribed period. We further measured test

https://doi.org/10.5194/egusphere-2023-2259
Preprint. Discussion started: 8 November 2023

thickness and treated the test as an elliptical cylinder to estimate sedimentation volume from the extension amount, extrapolating the density of calcium carbonate to estimate and approximate the amount of calcification.

2.2.1 Test Formation Observation by Differential Interference Contrast Microscope

Test growth was observed using an inverted DIC microscope (Axio Observer Z1, Zeiss, Germany). Time-lapse images were automatically captured by the digital microscope software Zen (version 2.0). Observations were conducted using a 100x objective lens Plan Achromat. The start and end frames of the time-lapse photography were overlaid using Photoshop. The length of the newly grown section of test was then measured using ImageJFiji (Schindelin et al., 2012).

2.2.2 Fluorescent Observation

To determine *S. vivipara* test growth in a 24-hour culture, fluorescent staining with Calcein was performed. Calcium carbonate fluorescent staining involved creating a 100 µM Calcein seawater solution and incubating it for 24 hours (Bernhard et al., 2004). Stained foraminifera were divided into two groups, those that were continually fed and those that were starved for three days, and then subjected to 24-hour calcium carbonate fluorescent staining. After staining, tap water was rapidly added to the Petri dishes to fix the samples. Observations were then made using a fluorescence microscope (Axio Observer Z1, Zeiss, Germany) with a GFP filter, and photographs were taken. The length of the newly grown section of test was then measured using ImageJFiji.

2.3 Test Cross-Section and Ultrastructure Observation

Samples for ultrastructural analysis were fixed using a fixative solution (3% paraformaldehyde, 0.3% glutaraldehyde, 2% NaCl in PBS buffer, pH7.8) and then stored in 2% glutaraldehyde at 4°C to prevent cellular morphological changes due to dehydration. Following the fixation, the samples were washed in filtered seawater and post-fixed for 2 hours at 4°C in 2% osmium tetroxide in filtered seawater. After the osmium fixation, the samples were washed with distilled water and then conductively stained by incubating in a 0.2% tannic acid solution (pH 6.8) for 30 minutes. They were subsequently washed again in distilled water and further incubated in a 1% osmium tetroxide solution for 30 minutes. Following the staining process, the samples were washed in distilled water and then subjected to an ethanol ascending series for dehydration. This was followed by substitution with isoamyl acetate and then critical point drying. The samples were coated with osmium using the OPC80 osmium coater (Filgen, Japan). Micro sectioning of the samples was performed using a gallium ion beam with the Helios G4 UX (Thermo Fisher Scientific, USA) FIB-SEM installed at JAMSTEC Yokosuka Headquarters, following the guidelines set in Nagai et al. (2018). Test thickness was measured using ImageJFiji (Schindelin et al., 2012).

To estimate calcification, the *S. vivipara* test was assumed to be a perfect cylinder to ~~aid estimating~~ the volume of calcite precipitated. The test size was measured using a FIB-SEM, which allowed us to estimate the volume of calcification by combining the test elongation rate and thickness. Assuming the density of the test to be the same as calcium carbonate (2.7 g/cm^3) allowed us to estimate the amount of calcification.

2.4 Statistical Analysis

Statistical analysis was conducted using Microsoft Excel (Ver 16.66.1). Pearson's product-moment correlation coefficient was applied to assess the relationships between several parameters. First, we examined the relationship between the length of the test grown in 20 minutes and the pre-growth maximum test diameter. Secondly, the association between the calcification rate derived from the length grown in 20 minutes and the pre-growth maximum test diameter was explored. We then analysed the correlation between the pre-dyeing maximum test diameter with Calcein and the length grown in 24 hours. Lastly, we investigated the link between the calcification rate derived from Calcein staining and the length grown in 24 hours.

3 Results

3.1 Short-Term Growth Observation: 20-Minute Study using DIC Microscopy

Differential interference contrast microscopy was utilised to observe *S. vivipara* over a 20-minute period (Fig. 1) (see Section "Video Supplement"). The observation demonstrated the progressive elongation of the apical portion of the *S. vivipara* test. The time-lapse observation revealed that *S. vivipara* extends its pseudopodia from the test in a foliated manner (compare Fig. 1A with 1B white arrow). The cell appears to elongate uniformly as a tube-like protrusion from the test (Fig. 1B). Additionally, the formation of pores during test growth was also confirmed on the dorsal side of the test (Fig. 1B "P"). By overlaying images from the beginning and end of the observation and measuring the length of the elongated difference, it was found that the test extended by an average of 2.69µm (SD=0.90µm) (Fig. 1C and Table 1). The fastest growth was 4.13µm over 20 minutes, while the slowest growth still resulted in an extension of 1.53µm.

3.2 Long-Term Growth Evaluation: 24-Hour Analysis with Calcein Staining

The newly formed test ~~section stained~~ with Calcein ~~from the *S. vivipara* fed group~~, ~~produced the observed emanating signals in~~ Figure 2. The newly formed test section ~~emanating these signals~~ exhibited an average growth of 100 µm over the 24-hour incubation period (Table 2). The fastest growth over 24 hours was 137.69 µm, while the slowest growth was 44.63 µm.

In a separate group, the *S. vivipara* that were starved for three days–did not yield any fluorescent signals from the test (Supplemental Fig. s1).

3.3 Analysis of Test Thickness, Dimensions, and Calcification

Measurements were taken for both the thickness of the tests and the long and short diameters of the tubular test using focused ion beam scanning electron microscopy (FIB-SEM) (Table 3, Table 4). The average test thickness was determined to be 1.008µm (SD 0.145µm), with observations indicating that the test was thicker on the ventral side compared to the dorsal side. The average dimensions for the major and minor axes of the test cross-sections were calculated to be 26.0 µm and 14.4 µm, respectively. Using these dimensions and the average growth of 99.39 µm in 24 hours, we calculated the volume of the test grown per day as 3,081 µm3. Considering the density of calcium carbonate (calcite) is 2.7 g/cm^3, we estimate that *S. vivipara* deposits 8.31 ng of calcium carbonate per day. During a 20-minute period, the average growth is 2.69µm, corresponding to a volume increase of 83.39µm^3, and the estimated precipitation of 0.23ng of calcium carbonate.

3.4 Individual Size and Test Growth

The correlation coefficient between the calcification rate determined from the length grown in 20 minutes and the maximum shell diameter before formation was r^2=0.13, indicating that the correlation was very weak. Pearson's product ratio correlation coefficient was determined and found to be p=0.92, not significantly different. The correlation coefficient of r^2=0.20 for the correlation between the rate of calcification and the length of growth at 24 hours, which was determined by Calcein staining, was very weak. Pearson's product ratio correlation coefficient was also obtained, p=0.99, and no significant difference was found. This indicates that the correlation between individual size, shell growth (i.e., length of shell formation), and calcification rate is very weak.

4 Discussion

4.1 Comparison of Calcification Rates

Calcification rates over a short timespan (20 minutes) were found to vary between 20~~0~~ and 55~~0~~ nmol/cm^2/min (Table 1). This was higher than the rates observed over a 24-hour time period (80–250 nmol/cm^2/min; Table 2). This discrepancy suggests that the addition of calcite by *S. vivipara* is episodical and that within a day, there are periods with and without chamber elongation. The relatively continuous calcite addition over the 20-minute observations likely provides the maximum deposition rates during test growth.

We also observed that calcification rates were not correlated to individual test sizes (Tables 1 and 2). The absence of test elongation when no food is present suggests that calcification is linked to the growth of the foraminiferal cell. Hohenegger (2018) speculated that the timing of chamber construction is correlated with the cell's growth patterns and showed that in linearly growing cell volumes, the chamber building rate aligns consistently with the growth rate. This consideration aligns with the growth pattern of *S. vivipara* in our study which, despite its curved nature, essentially follows a pattern of increasing tube length. ~~It may well be that~~ calcification ~~is~~ a response to the cell's increased volume increasing beyond that of the spirillinid's tubular chamber.

The maximum calcification rates for *S. vivipara* were higher than those of other foraminiferal species or inorganic precipitation experiments~~, as shown in Table 3.~~ Due to their overall small size, the high rates in this taxon do not necessarily result in much calcium carbonate production per individual. By normalizing the calcium carbonate formation rate per unit area, *S. vivipara* shows the highest calcium carbonate precipitation rates amongst all studied species, as well as compared to rates found in most inorganic precipitation experiments. To further clarify these results, we compared the calcification rate of *S. vivipara* with those reported in various other taxa (Table 5).

https://doi.org/10.5194/egusphere-2023-2259
Preprint. Discussion started: 8 November 2023

The notably fast carbonate deposition rate per unit area observed in *S. vivipara* is believed to be intrinsically linked to its test formation strategy. ~~In~~ foraminiferal chamber formation, an organic mold is formed and acts as a substrate upon which the new chamber's hard material (calcium carbonate) is transported to, and built upon, ensuring the desired chamber morphology. While calcification typically occurs across the entirety of a newly forming chamber, *S. vivipara* initiates crystalline growth solely at the test aperture's tip. As a result, the calcification site is restricted, leading to a straightforward transportation path for the chamber's materials from seawater. This could explain the swift carbonate deposition rates. The minimised calcification amount per individual may also play a role. Essentially, with the calcification site being small, ~~it's~~ possible that the ~~concentrated~~ energy and material resources result in faster calcification rates. While there are no studies specifically addressing the effect of the size of calcification sites on the rate of carbonate deposition, there is a related example regarding planktonic foraminiferal spines with apical growth rates ranging from ~0.7µm min-1 to a maximum of ~8µm min-1 (Izumida et al., 2022). The precise mechanisms and reasons ~~for~~ why a smaller calcification site might promote faster precipitation remain unclear based on current knowledge. Hence, a deeper understanding of foraminiferal ~~logistics,~~ particularly in how calcium and other calcareous test materials are transported and deposited, is imperative for future research.

Building on this, according to Blackmon and Todd (1959), the *S. vivipara* test contains a high magnesium concentration of 17 mol%, equivalent to a Mg/Ca ratio of 170 mmol/mol. While many planktonic foraminifera and benthic foraminifera like *Cibicidoides* and *Ammonia* exhibit Mg/Ca ratios in the range of 1–4 mmol/mol, species such as Miliolid, Calcarinidae, and *Planograbratella* ~~surpass~~ 100 mmol/mol, classifying them as High-Mg calcite species. Notably, *S. vivipara* can be included within this High-Mg ~~criteria~~ (Toyofuku et al., 2000; James and Austin, 2008; Toyofuku et al., 2011; De Bar et al., 2019). When applied to the TMT-PT model that explains calcium transport in foraminiferal calcification, such a high magnesium concentration can be attributed more to Passive Transportation (deriving seawater as the source of calcium carbonate) than Trans Membrane Transportation, which selectively absorbs calcium (Nehrke et al., 2013). To clarify these points in the future, approaches like pH and Ca imaging, microscopic observations of the growing shell front, and detailed multi-element chemical composition analyses are essential.

▪ 4.2 Implications for Species' Life Cycle and Ecology

Considering our findings, it becomes evident that the unique test formation of *S. vivipara* is deeply rooted in its ecological ~~tactics~~ and evolutionary advancements. The distinct continuous coiled chamber design, setting it apart from other chambered whorl tests of Rotaliid foraminifera, combined with its notably ~~brief~~ life span, ~~underscores~~ a specialized survival mechanism (Myers, 1936; Lee and Anderson, 1991; Goldstein, 2003). Such a mechanism not only traces the evolutionary path of *S. vivipara* but also reveals its ~~capacity~~ to adapt its cell volume swiftly by precipitating tests at an unparalleled rate.

~~*Spirillina. vivipara's* swift growth~~ may present additional ecological advantages by enabling ~~the~~ species to colonise diverse environments and secure ecological niches. Documented mainly as epifauna on continental shelves (Murray, 2006), *S. vivipara*'s rapid growth rate and propagule-based dispersal mechanism likely provide a strategic advantage for swift maturation and life cycle completion (Murray, 2013). *Spirillina vivipara* is distributed along the western side of both the North and South Pacific Oceans, its marginal seas, the coasts of the North Atlantic Ocean on both the eastern and western sides, including the Gulf of Mexico, the coastal regions of the Mediterranean Sea and the Indian Ocean (Hayward, 2023; Obis, 2023). In all these locations, consistent with Murray (2013), the ecological behaviour of rapid growth even when individual specimen size is small, seems to provide an advantage in ~~securing~~ ecological space. The unique reproduction process of *S. vivipara*, including the timing of sexual and asexual reproduction, greatly influences its growth rate. The minimum time required to complete both the sexual and asexual reproductive stages in *S. vivipara* is approximately 18 days (Myers, 1936). Our research ~~found~~ the shortest period for these stages within our study sample to be 7–10 days, resulting in an overall life cycle of approximately 14–20 days (Nagai, unpublished data). As cell volume increases, the number of progeny produced during gametogenesis correspondingly escalates, leading to a larger dispersal of offspring. In fact, the cosmopolitan distribution of this taxon indicates the success of this type of dispersal strategy in expanding distribution, and the rapid growth rate may be a factor facilitating this.

5 Summary

Our investigation into the calcification and growth rates of the benthic foraminifera, *Spirillina vivipara*, has provided distinctive insights into its test growth characteristics. Through time-lapse imaging and the use of Calcein to confirm calcium incorporation into the test, this study has laid the groundwork for potential further investigations into the other elemental uptakes within foraminiferal calcite. Future research into the nature of this elemental uptake holds the potential to shed light on elemental distribution in cases of rapid calcification. Such studies could enhance our understanding of the ecology of foraminifera and their implications for paleoclimate reconstructions. Therefore, further attention to the elemental composition of *S. vivipara* is warranted. The crystalline properties of such rapid test formation are also of great interest. Comprehensive crystallographic analysis of *S. vivipara* in future research could help reveal its unique calcification mechanisms. Advanced techniques, such as electron backscatter diffraction (EBSD) and transmission electron microscopy (TEM), to determine crystal orientation, might uncover more detailed ~~aspects~~ of the test's structure and composition. In conclusion, this study emphasizes the significance of understanding the growth and calcification of foraminiferal tests on a species-specific basis. Such insights can influence not only our knowledge of foraminiferal ecology but also the wide-ranging roles of foraminifera in marine carbon cycling and paleoclimate research, thereby ~~carrying~~ extensive implications.

Acknowledgments

We thank Nanami Kishigami, Yuki Iwadate, and Sunao Kubo for their help in stock culturing foraminifera, Remi Tsubaki, Jelle Bijma, and Lennart de Nooijer for their scientific advice. We would like to thank Makoto Sugimura, Yuka Toyoda-

Koyano and Ayuta Shinozaki of Shin Enoshima Aquarium for their cooperation in collecting foraminifera. This work was supported by JSPS KAKENHI 19K21197, 21K14035, 23H00339, 23K03568 and JST Grant Number JPMJPF2104.

Author Contributions

YN and TT both equally contributed as co-first authors, conceiving and designing the study, conducting animal husbandry, observations, data analysis, and playing a major role in writing and constructing the manuscript. BM was responsible for identifying the species, validating the discussion, and contributing to the writing process. KU handled preprocessing and observations using the electron microscope. All authors reviewed and approved the final manuscript.

Video supplement

Time-lapse videos show *S. vivipara* forming a test within 20 minutes. Supplementary Movie 1: S. *vivipara* forming a test within 20 minutes observed from the dorsal side. The formation of pores at the apical portion can also be observed. The video can be accessed at https://doi.org/10.5446/63152.

Supplementary Movie 2: S. *vivipara* forming a test within 20 minutes observed from the ventral side. The video can be accessed at https://doi.org/10.5446/63153.

Table 1: Average *S. vivipara* test growth over 20 minutes..

Sample ID	Maximum Test Diameter (µm)	Elongated Length(µm) in 20 min	Standard Deviation	Measurement number	Length per hour(µm)	nmol/cm2/min
A	nd	3.39	0.53	11	10.167	457
B	nd	2.46	0.24	10	7.3932	333
C	73.79	4.13	0.49	10	12.4023	558
D	70.62	2.82	0.27	10	8.454	380
E	nd	1.53	0.17	10	4.5813	206
F	76.04	1.77	0.23	10	5.2992	238
G	nd	2.75	0.36	10	8.2647	372
Average	73.48	2.69	0.9		8.08	364±242

https://doi.org/10.5194/egusphere-2023-2259
Preprint. Discussion started: 8 November 2023

Table 2: Average test growth in 24 hours.

Sample ID	Maximum Test Diameter (µm)	Elongated Length(µm) in 24 hours	Standard Deviation	Measurement number	Length per hour(µm)	nmol/cm2/min
H	166.82	113.36	12.08	3	4.72	212
I	93.42	60.34	12.45	4	2.51	113
J	161.54	137.69	nd	2	5.74	258
K	103.77	132.42	49.48	3	5.52	248
L	89.15	126.48	40.24	3	5.27	237
M	88.61	80.8	23.98	3	3.37	151
N	102.53	44.63	5.81	3	1.86	84
Average	115.12	99.39	37.32		4.14	186±140

250 **Table 3: Average *S. vivipara* test thickness from cross sectional measurements.**

Sample ID	Thickness (µm)
O	1.0
P	1.0
Q	0.8
R	1.2
Average	1.0
SD	0.15

Table 4: Measured long and short (B) test axes of *S. vivipara*.

Specimen	Long axes (µm)	Short axes (µm)
S	26.3	17
T	22.7	13
U	25.2	15.7
V	22.8	11.3
W	29.3	14.4
X	29.7	15.1
Average	26	14.4
SD	1.9	2.0

Table 5: Comparison of calcification rate of *S. vivipara* with previously reported data of foraminifera and inorganic precipitation experiments.

Measured Item	Calcification Rate	Reference
Spirillina vivipara Ehrenberg, 1843	0.0067 nmol/hr	This study
Archaias angulatus (Fichtel and Moll, 1798)	2.0–42 nmol/hr	Duguay and Taylor, 1978
Trilobatus. sacculifer (Brady, 1877)	0.032–1.1 nmol/hr	Erez, 1982
	2.6–3.9 nmol/hr	Anderson and Faber, 1984
Amphistegina spp.	1.7–23 nmol/hr	ter Kuile and Erez, 1984
Ammonia tepida (Cushman, 1926)	0.28 nmol/hr	Glas et al., 2012
When Calcification rate is normalized per unit area per minute		
Spirillina vivipara Ehrenberg, 1843	364±242 nmol/cm^2/min	This study
Ammonia confertitesta Zheng, 1978	~24±5 nmol/cm^2/min	Geerken et al, 2022
Planktonic species	~0.6–80 nmol/cm$^{2/}$min	Erez and Luz, 1983; Anderson and Faber, 1984
Benthic species	~1.33–430 nmol/cm^2/min	Erez and Luz, 1983; Anderson and Faber, 1984
Inorganic (seawater)	0.06–8.5 nmol/cm^2/min	Erez and Luz, 1983; Anderson and Faber, 1984
Inorganic (Mg-free)	0.16–90 nmol/cm^2/min	Tesoriero and Pankow, 1996; Nehrke et al., 2007; Tang et al., 2012

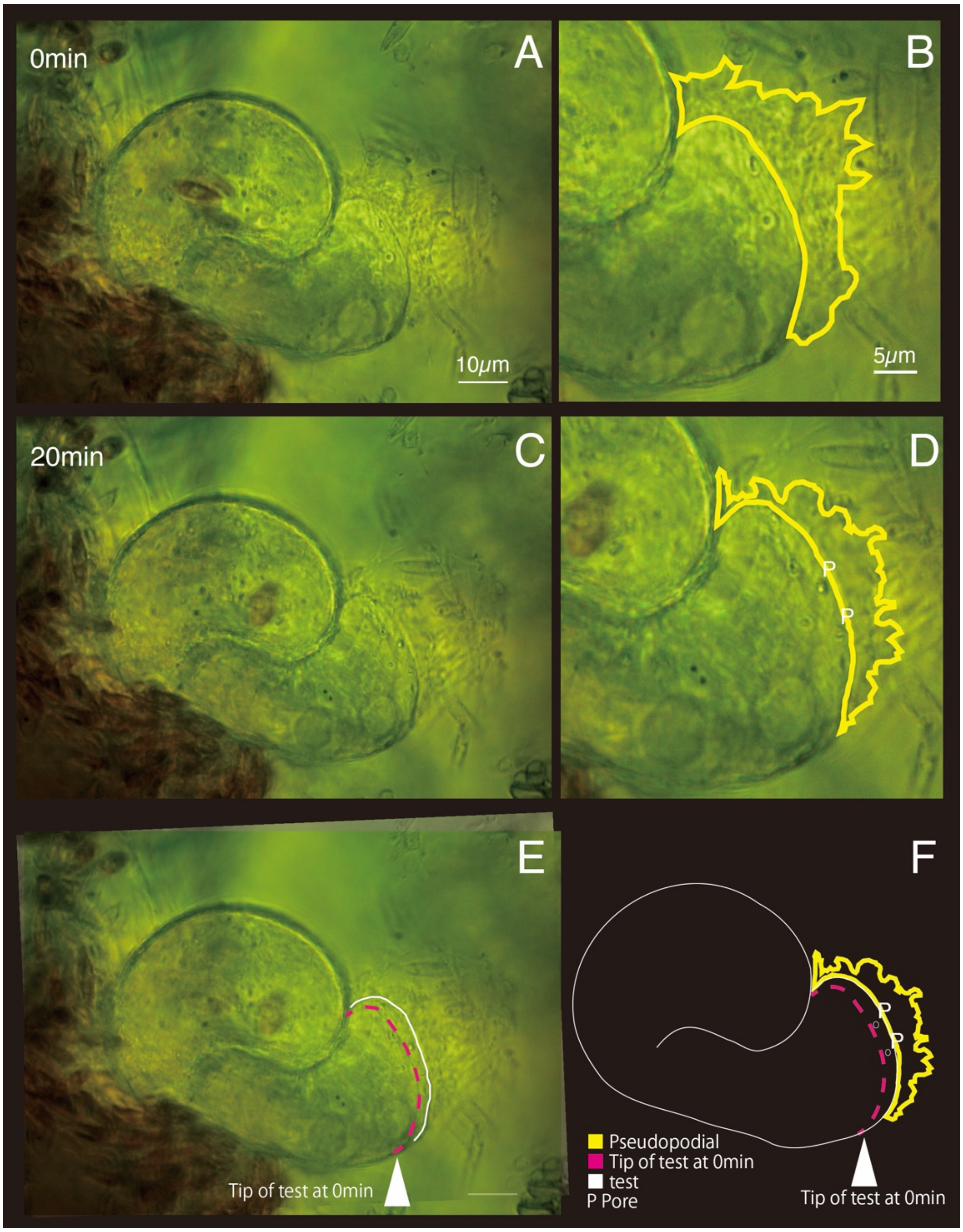

Figure 1: Superimposed images of two micrographs taken at different time points. A: 0 minutes. B: Pores and pseudopodial distribution are illustrated in the magnified image at 0 minutes. C: 20 minutes. D: Newly constructed pores (P) and pseudopodial distributions. E: Overlapping image of A (0 min) and C (20 min). F: Sketch made by overlaying the images taken at 0 min and 20 min. In E and F, the white arrowhead and magenta dotted line show the test front at 0 min, and the white solid line shows the test front at 20 min.

https://doi.org/10.5194/egusphere-2023-2259
Preprint. Discussion started: 8 November 2023

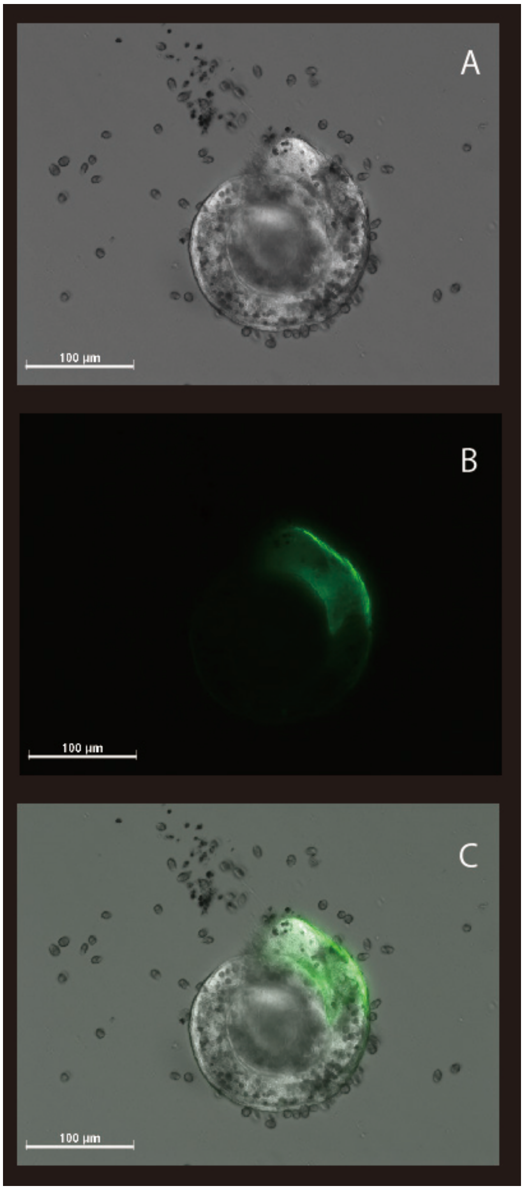

Figure 2: Sites stained by Calcein (a green fluorescent calcium indicator) during the 24-hour observation period. (a) Differential Interference Contrast (DIC) image, (b) Fluorescence image, (c) Overlay of images (a) and (b). The scale bar represents 100µm.

https://doi.org/10.5194/egusphere-2023-2259
Preprint. Discussion started: 8 November 2023

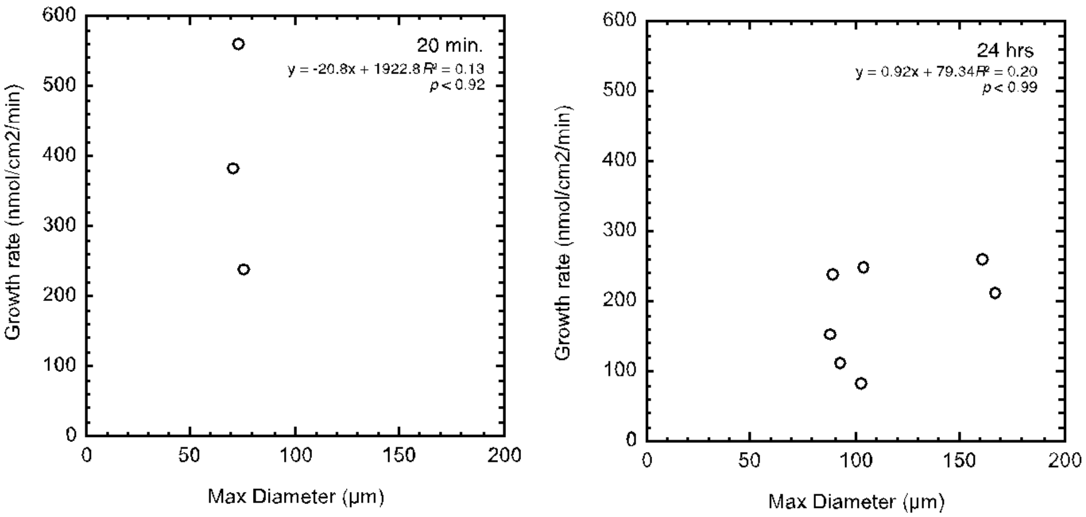

Figure 3: The comparison between the size of the individuals and the growth rate: a) in 20 min. b) in 24 hours. Note that for some individuals, only the growth area was recorded during microscope observation instead of capturing the entire individual.

https://doi.org/10.5194/egusphere-2023-2259
Preprint. Discussion started: 8 November 2023

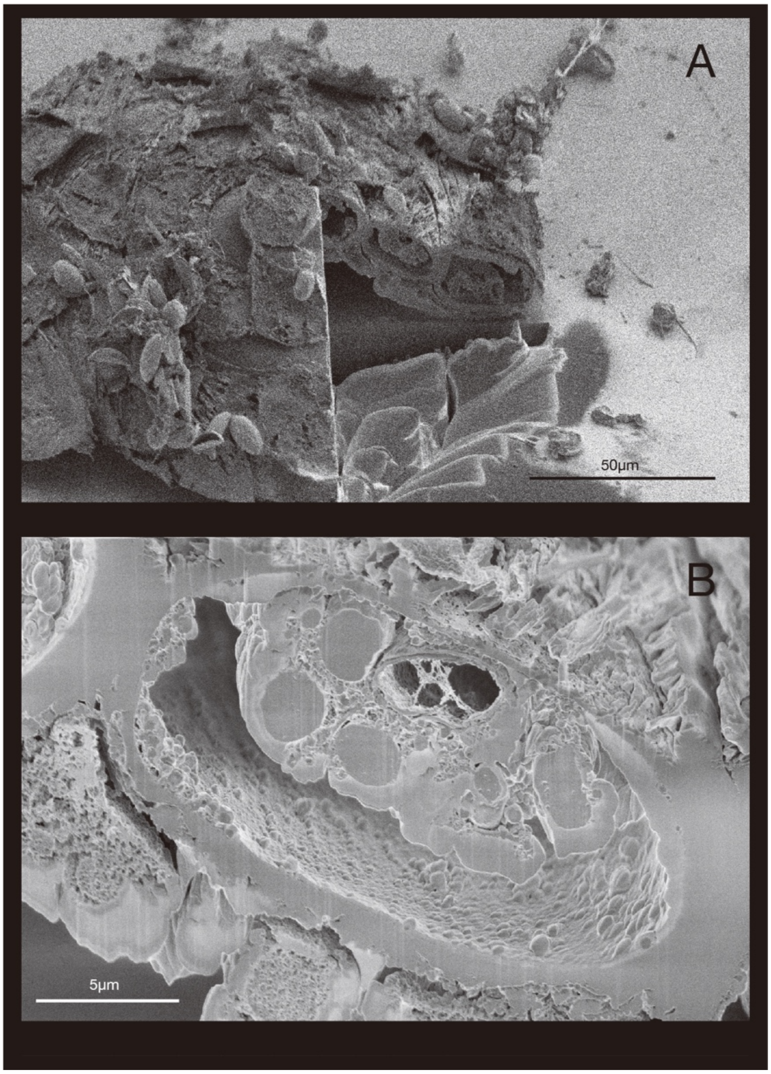

Figure 4: Transverse section of a shell of *S. vivipara* micromachined by FIB. The cross section of the test is nearly elliptical and tubular.

References

Alve, E. and Goldstein, S. T.: Dispersal, survival and delayed growth of benthic foraminiferal propagules, J. Sea Res., 63, 36-51, https://10.1016/j.seares.2009.09.003, 2010.

Anderson, O. R. and Faber, W. W.: An estimation of calcium carbonate deposition rate in a planktonic foraminifer *Globigerinoides sacculifer* using ^{45}Ca as a tracer; a recommended procedure for improved accuracy, J. Foraminifer. Res., 14, 303-308, https://10.2113/gsjfr.14.4.303, 1984.

Bernhard, J., Blanks, J. K., Hintz, C. J., and Chandler, G. T.: Use of the fluorescent calcite marker calcein to label foraminiferal tests, J. Foraminifer. Res., 34, 96-101, https://doi.org/10.2113/0340096, 2004.

Brady, H. B.: Supplementary note on the foraminifera of the Chalk of the New Britain group, Geol. Mag. n. ser. 4, 534–536, 1877.

Cheng, T. and Zheng, S. Y.: The recent foraminifera of the Xisha Islands, Guandong Province, China I, Studia Marina Sinica 12, 149–266, 1978.

Cushman, J. A.: Foraminifera of the typical Monterey of California, Contr. Cushman Lab. Forum. Res. 2, 53–69, 1926.

de Bar, M. W., de Nooijer, L. J., Schouten, S., Ziegler, M., Sluijs, A., and Reichart, G.-J.: Comparing Seawater Temperature Proxy Records for the Past 90 Myrs From the Shallow Shelf Record Bass River, New Jersey, Paleoceanogr. and Paleoclimatol., 34, 455-475, https://doi.org/10.1029/2018PA003453, 2019.

Duguay, L. E. and Taylor, D. L.: Primary Production and Calcification by the Soritid Foraminifer *Archais angulatus* (Fichtel & Moll)*, J. Protozool., 25, 356-361, https://doi.org/10.1111/j.1550-7408.1978.tb03903.x, 1978.

Ehrenberg, C.G.: Verbreitung und Einfluss des Mikroskopischen Lebens in Süd-und Nord Amerika, Physikalische Abhandlungen der Königlichen Akademie der Wissenschaften zu Berlin, 1841 Theil 1, 291–446, 1843.

Erez, J. and Luz, B.: Temperature control of oxygen-isotope fractionation of cultured planktonic foraminifera, Nature, 297, 220-222, https://doi.org/10.1038/297220a0, 1982.

Fichtel, L. and Moll, J. P. C.: Testacea microscopica aliaque minuta ex generibus Argonauta et Nautilis ad naturam picta et descripta, Camesina, Vienna, 1798.

Geerken, E., de Nooijer, L., Toyofuku, T., Roepert, A., Middelburg, J. J., Kienhuis, M. V. M., Nagai, Y., Polerecky, L., and Reichart, G.-J.: High precipitation rates characterize biomineralization in the benthic foraminifer *Ammonia beccarii*, Geochim. Cosmochim. Acta, 318, 70-82, https://doi.org/10.1016/j.gca.2021.11.026, 2022.

Glas, M. S., Langer, G., and Keul, N.: Calcification acidifies the microenvironment of a benthic foraminifer (*Ammonia* sp.), J. Exp. Mar. Biol. Ecol., 424-425, 53-58, https://doi.org/10.1016/j.jembe.2012.05.006, 2012.

Goldstein, S. T.: Foraminifera: A biological overview, in: Modern Foraminifera, Springer Netherlands, Dordrecht, 37-55, https://doi.org/10.1007/0-306-48104-9_3, 2003.

Hayward, B.W.; Le Coze, F.; Vachard, D.; Gross, O. (2023). World Foraminifera Database. Accessed at https://www.marinespecies.org/foraminifera on 2023-08-03. https://doi.org/10.14284/305

Hohenegger, J.: Foraminiferal growth and test development, Earth-Sci. Rev., 185, 140-162, https://doi.org/10.1016/j.earscirev.2018.06.001, 2018.

Izumida, K., Takasaki, M., Fujimaki, R., Nagai, Y., Oaki, Y., Naito, K., Tanaka, Y., Shimode, S., Toyofuku, T., and Imai, H.: Characterization of calcite spines of planktonic foraminifers (Globigerinidae), CrystEngComm, 24, 2446-2450, https://doi.org/10.1039/D2CE00110A, 2022.

James, R. H. and Austin, W. E. N.: Biogeochemical controls on palaeoceanographic environmental proxies: a review, Geol. Soc. Lond. Spec. Publ., 303, 3-32, https://doi.org/10.1144/SP303.2, 2008.

Langer, M. R.: Assessing the Contribution of Foraminiferan Protists to Global Ocean Carbonate Production1, J. Eukaryot. Microbiol., 55, 163-169, https://doi.org/10.1111/j.1550-7408.2008.00321.x, 2008.

Langer, M. R., Silk, M. T., and Lipps, J. H.: Global ocean carbonate and carbon dioxide production; the role of reef Foraminifera, J. Foraminifer. Res., 27, 271-277, https://doi.org/10.2113/gsjfr.27.4.271, 1997.

Lee, J. J. and Anderson, O. R.: Biology of the foraminifera, Academic Press, London UK, 368pp, 1991.

Loeblich, A. R. and Tappan, H. N.: Foraminiferal genera and their classification, Van Nostrand Reinhold Co., New York USA, 1728pp, 1987.

Murray, J. W.: Ecology and applications of benthic foraminifera, Cambridge University Press, Cambridge UK, 426 pp., https://doi.org/10.1017/CBO9780511535529, 2006.

Murray, J. W.: Living benthic foraminifera: biogeographical distributions and the significance of rare morphospecies, J. Micropalaeontol., 32, 1-58, https://doi.org/10.1144/jmpaleo2012-010, 2013.

Myers, E. H.: The life-cycle of *Spirillina vivipara* Ehrenberg, with notes on morphogenesis, systematics and distribution of the Foraminifera, J. R. Microsc. Soc., 56, 120-146, https://doi.org/10.1111/j.1365-2818.1936.tb01509.x, 1936.

Nagai, Y., Uematsu, K., Wani, R., and Toyofuku, T.: Reading the Fine Print: Ultra-Microstructures of Foraminiferal Calcification Revealed Using Focused Ion Beam Microscopy, Front. Mar. Sci., 5, 67, https://doi.org/10.3389/fmars.2018.00067, 2018.

Narayan, G. R., Reymond, C. E., Stuhr, M., Doo, S., Schmidt, C., Mann, T., Westphal, H., and Mateu-Vicens, G.: Response of large benthic foraminifera to climate and local changes: Implications for future carbonate production, Sedimentology, 69, 121-161, https://doi.org/10.1111/sed.12858, 2021.

Nehrke, G., Reichart, G. J., Van Cappellen, P., Meile, C., and Bijma, J.: Dependence of calcite growth rate and Sr partitioning on solution stoichiometry: Non-Kossel crystal growth, Geochim. Cosmochim. Acta, 71, 2240-2249, https://doi.org/10.1016/j.gca.2007.02.002, 2007.

Nehrke, G., Keul, N., Langer, G., de Nooijer, L. J., Bijma, J., and Meibom, A.: A new model for biomineralization and trace-element signatures of Foraminifera tests, Biogeosciences, 10, 6759-6767, https://doi.org/10.5194/bg-10-6759-2013, 2013.

OBIS: Ocean Biodiversity Information System, https://obis.org/taxon/113737, last access; 1 September 2023.

Schindelin, J., Arganda-Carreras, I., Frise, E., Kaynig, V., Longair, M., Pietzsch, T., Preibisch, S., Rueden, C., Saalfeld, S., Schmid, B., Tinevez, J.-Y., White, D. J., Hartenstein, V., Eliceiri, K., Tomancak, P., and Cardona, A.: Fiji: an open-source platform for biological-image analysis, Nat. Methods, 9, 676-682, https://doi.org/10.1038/nmeth.2019, 2012.

Tang, J., Niedermayr, A., Köhler, S. J., Böhm, F., Kısakürek, B., Eisenhauer, A., and Dietzel, M.: Sr^{2+}/Ca^{2+} and $^{44}Ca/^{40}Ca$ fractionation during inorganic calcite formation: III. Impact of salinity/ionic strength, Geochim. Cosmochim. Acta, 77, 432-443, https://doi.org/10.1016/j.gca.2011.10.039, 2012.

ter Kuile, B. and Erez, J.: In situ growth rate experiments on the symbiont-bearing foraminifera *Amphistegina lobifera* and *Amphisorus hemprichii*, J. Foraminifer. Res., 14, 262-276, https://doi.org/10.2113/gsjfr.14.4.262, 1984.

Tesoriero, A. J. and Pankow, J. F.: Solid solution partitioning of Sr^{2+}, Ba^{2+}, and Cd^{2+} to calcite, Geochim. Cosmochim. Acta, 60, 1053-1063, https://doi.org/10.1016/0016-7037(95)00449-1, 1996.

Toyofuku, T., Kitazato, H., Kawahata, H., Tsuchiya, M., and Nohara, M.: Evaluation of Mg/Ca thermometry in foraminifera: Comparison of experimental results and measurements in nature, Paleoceanography, 15, 456-464, https://doi.org/10.1029/1999PA000460, 2000.

Toyofuku, T., Suzuki, M., Suga, H., Sakai, S., Suzuki, A., Ishikawa, T., de Nooijer, L. J., Schiebel, R., Kawahata, H., and Kitazato, H.: Mg/Ca and $\delta^{18}O$ in the brackish shallow-water benthic foraminifer *Ammonia 'beccarii'*, Mar. Micropaleontol., 78, 113-120, https://doi.org/10.1016/j.marmicro.2010.11.003, 2011.